Continuous-wave and ultrafast coherent reflectivity studies of excitons in bulk GaN

O. Aoudé,[1] P. Disseix,[1] J. Leymarie,[1] A. Vasson,[1] M. Leroux,[2] E. Aujol,[3] B. Beaumont,[3] A. Trassoudaine,[1] and Y. André[1]
[1]*LASMEA UMR 6602 UBP/CNRS, 24 Avenue des Landais, F-63177 Aubière Cedex, France*
[2]*CRHEA-CNRS, Rue Bernard Grégory, 06560 Valbonne, France*
[3]*LUMILOG, 2720 Chemin de Saint Bernard, F-06222 Vallauris, France*
(Received 21 December 2006; revised manuscript received 18 October 2007; published 16 January 2008)

We report an extensive study of the excitonic properties of freestanding and heteroepitaxial GaN samples using continuous-wave reflectivity and time-resolved autocorrelation measurements. The coherent impulse response of free excitons is recorded by using an interferometric correlation technique. Excitonic parameters of GaN are deduced from the combined analysis of both experiments. Oscillator strengths and transition energies are studied as a function of the residual biaxial strain of the sample and temperature-dependent measurements are used to determine the parameters of the exciton-phonon interaction in GaN.

DOI: 10.1103/PhysRevB.77.045206 PACS number(s): 78.20.−e, 71.35.−y, 78.47.−p, 78.55.Cr

I. INTRODUCTION

GaN crystallizing in the hexagonal wurtzite structure and related compounds have been intensively studied due to their recognized potential for device applications in short-wavelength optoelectronics and in high-frequency or high-temperature electronics.[1–3] An in depth understanding of their fundamental properties is then essential in order to design optimized devices but also to fully investigate their potential for novel optoelectronic devices such as ultrafast micro-optical amplifiers[4,5] or polariton light emitters.[6] In particular, the spectroscopy of excitons provides relevant information of basic and applied interest. It is well known that excitons dominate the near-band-edge optical properties of GaN.[7,8] They are characterized by large binding energies and oscillator strengths, allowing them to be stable at high temperature or high density. Consequently, the strong light-matter coupling and large Rabi splittings have been predicted[9] and recently demonstrated at low and room temperatures in GaN-based microcavities.[10–12] It is now expected that this strong coupling regime will be crucial for a new generation of GaN-based light emitters with very low thresholds. It is important to optimize the design of GaN microcavities in order to further investigate the physics of the strong coupling regime. It is also necessary to determine accurately the excitonic oscillator strengths of GaN as a function of the residual biaxial strain which strongly varies with the growth process.

The effect of disorder on the optical properties of excitons in nitrides, which is mainly attributed to the inhomogeneous distribution of the lattice strain, is also an important issue. Strain fluctuations manifest themselves in both continuous-wave (cw) and time-resolved spectroscopies and are typically responsible for the inhomogeneous broadening of the transitions which combines with the homogeneous broadening when the temperature increases. This leads to a mixed Lorentzian-Gaussian shape of the exciton line and a partial breakdown of the temporal coherence.

In this context, the excitonic optical properties of various GaN samples are examined in this work by combining both cw and time-resolved reflectivity experiments. Nevertheless, due to the short coherent transient of excitons in GaN,[13] exciton dynamics have to be analyzed at the femtosecond scale. We show that excitonic reflectivity transients of bulk GaN can be accurately recorded by means of an interferometric correlation method already proposed for the GaAs/GaAlAs system.[14–16] The excitonic oscillator strength and broadening are derived from the best fits of both cw and time-resolved spectra. The inhomogeneous broadening parameters are derived from the decay rate of the low-temperature correlation signal without affecting the accuracy of the determination of the oscillator strength as it could be the case if only cw data are fitted. Energies and oscillator strengths of excitons are then analyzed as a function of the in-plane biaxial strain of the samples and compared with calculations. Moreover, the homogeneous broadening has been evaluated as a function of temperature by using complementary temperature-dependent cw-reflectivity and time-resolved correlation experiments. This homogeneous broadening of excitons is then analyzed in terms of scattering by acoustic and optical phonons or by ionized donor impurities.

II. EXPERIMENTAL DETAILS AND THEORETICAL CONSIDERATIONS

All the samples investigated in this study are unintentionally doped bulk GaN epilayers. Their main characteristics are reported in Table I: thickness of the layer, dislocation density, and growth technique used for their elaboration. Four of them labeled S_3 to S_6 are thick freestanding samples grown by hydride vapor phase epitaxy (HVPE). Sample S_2 is a 3 μm thick GaN layer grown by metal-organic vapor phase epitaxy (MOVPE) on a (0001) sapphire substrate. Sample S_1 was grown by using an epitaxial lateral overgrowth (ELOG) process: A few micrometer thick GaN layer was first grown by MOVPE on a (0001) Al_2O_3 substrate; a dielectric (Si_xN_y) mask was then deposited and stripes were opened using standard photolithography; finally, regrowth of GaN was performed in the openings taking advantage of the lateral growth over the mask up to full coalescence. This technique significantly reduces the dislocation density of GaN layers.[17,18] The last sample (S_7) is a 110 μm thick GaN ep-

TABLE I. Description of the investigated samples with their corresponding labels.

Samples	Structure	Thickness (μm)	Growth technique	Dislocation density (cm^{-2})
S_1	GaN/sapphire	12	ELOG	10^8
S_2	GaN/sapphire	3	MOVPE	
S_3	Freestanding	300–350	HVPE	10^6-10^7
S_4	Freestanding	300–350	HVPE	10^6-10^7
S_5	Freestanding	1100	HVPE	10^6-10^7
S_6	Freestanding	400–550	HVPE	10^6-10^7
S_7	GaN/GaN	110	ELOG, HVPE	

ilayer regrown by HVPE on an ELOG GaN template elaborated in the same conditions as S_1.

The optical experiments were performed in the 5–300 K range. The excitation source for cw reflectivity is a halogen lamp and the reflectivity signal is analyzed through a monochromator using standard lock-in techniques. For the time-resolved reflectivity experiments, the second-harmonic beam of a femtosecond Ti:sapphire laser with 130 fs pulse duration and 76 MHz repetition rate is used. The light pulse is passed through a Michelson interferometer providing two collinear pulses which are then focused on the sample with a mutual delay τ. The photon energy is chosen to be equal to the average value of the $X_A^{n=1}$ and $X_B^{n=1}$ exciton energies of GaN. The coherent reflectivity transient is then probed as a function of τ by the time integrated detection of the reflected signal with a Si photodiode. A detailed schematic view of the interferometric correlation setup can be found in Ref. 19. The intensity of the time integrated signal is proportional to

$$I(\tau) \propto \int |r(t) + r(t-\tau)|^2 dt, \tag{1}$$

where $r(t)$ is the time-resolved reflection amplitude coefficient. This expression can be rewritten as $I(\tau)=2[I_0+I_{rr}(\tau)]$ where $I_0=\int|r(t)|^2dt=\int|r(t-\tau)|^2dt$ is constant and $I_{rr}(\tau)=\int \mathrm{Re}[r(t)r^*(t-\tau)]dt=\mathrm{Re}[r(\tau)\otimes r^*(-\tau)]$ is the autocorrelation function of $r(t)$. It can be shown that this autocorrelation function is very close to the time-resolved reflection coefficient $r(t)$.[20] Our experiments were performed under normal incidence so that the electric field and the wave vector of light were, respectively, perpendicular and parallel to the (0001) axis (c axis) of the samples.

The cw and time-resolved reflectivity spectra were analyzed by modeling the optical response using a standard transfer-matrix algorithm. The dielectric constant in the vicinity of the band edge is given in a semiclassical approach by

$$\varepsilon(E) = \varepsilon_b + \sum_{j=1}^{N} \int \frac{A_j}{(x^2 - E^2 + i\gamma_j E)} f(x, E_{0j}, \sigma_j) dx, \tag{2}$$

where ε_b is the background dielectric constant, and A_j, E_{0j}, and γ_j are, respectively, the oscillator strength, the mean resonance energy, and the homogeneous broadening parameter of the j excitonic level. The exciton resonance energies are assumed to follow a Gaussian distribution:

$$f(x, E_{0j}, \sigma_j) = \frac{1}{\sqrt{2\pi}\sigma_j} \exp \frac{(x - E_{0j})^2}{2\sigma_j^2}, \tag{3}$$

where σ_j is the inhomogeneous broadening parameter, related to microscopic disorder such as lattice strain fluctuations.

The time-resolved reflection coefficient $r(t)$ is calculated from the Fourier transform of the frequency-dependent coefficient $r(\nu)$ times a Gaussian function $g(\nu)$, corresponding to the spectral dispersion of the 130 fs pulse:

$$r(t) = \int r(\nu) g(\nu) e^{-i2\pi\nu t} d\nu. \tag{4}$$

The autocorrelation function $I_{rr}(\tau)$ is then numerically evaluated in order to calculate the interferometric signal $I(\tau)$ according to Eq. (1).

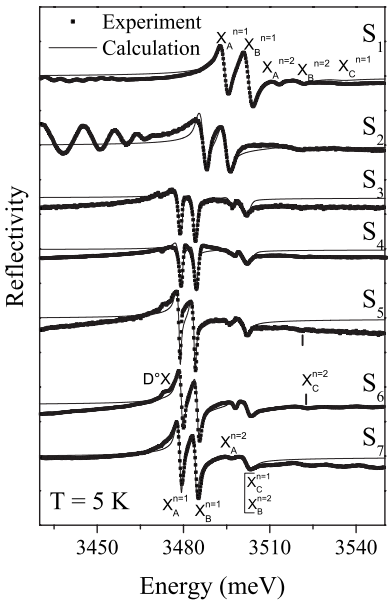

FIG. 1. 5 K reflectivity spectra of the investigated samples. The thin lines are fits to the experimental spectra.

III. RESULTS AND DISCUSSION

A. Low-temperature results

The 5 K cw-reflectivity spectra of the S_1 to S_7 samples are displayed in Fig. 1 together with their corresponding simulations. The spectra have been organized by ascending internal strain, S_1 corresponding to the most compressed sample. The A, B, and C free excitons related to the three valence bands of wurtzite GaN are clearly identified together with lines attributed to their $n=2$ excited states. The sharpness of the resonances indicates the high quality of the samples investigated. Within the hydrogen model, the binding energies (R) of the three excitons can be deduced from the energy spacing between $n=1$ and $n=2$

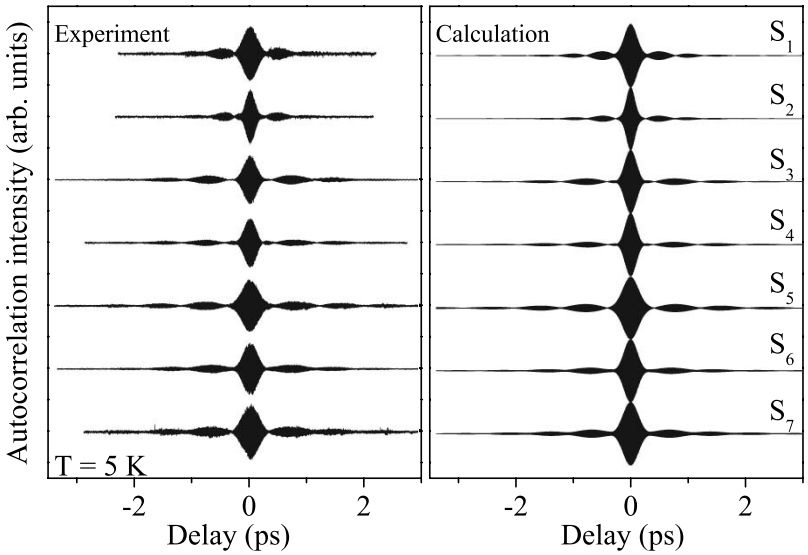

FIG. 2. Low-temperature experimental and calculated time-resolved autocorrelation spectra of the samples studied.

states giving $R_A=24.2\pm0.2$ meV, $R_B=25.9\pm0.2$ meV, and $R_C=25.9\pm0.2$ meV. A weak structure on the low energy side of the A exciton can be also detected and attributed to neutral donor bound excitons, although the reflectivity is mainly sensitive to intrinsic states. Photoluminescence experiments (not reported here) confirm this identification.

Figure 2 displays the corresponding experimental ($T=5$ K) and simulated time-resolved autocorrelation spectra of the samples studied. The laser energy was tuned to the average value of the A and B exciton energies. In these conditions, the latter are excited simultaneously since the temporal width of the femtosecond pulse (130 fs) corresponds to a spectral width of 14 meV, while the A-B splitting is 5–8 meV in our samples. A good agreement is obtained between experiments and calculations. The experimental interferograms show rapid oscillations corresponding to the interferences between the two coherent polarization waves excited by the pulses. These are not resolved on the time scale of Fig. 2. All the experimental spectra show a clear modulation of the overall signal corresponding to the quantum beats between the A and B excitons, simultaneously excited by each pulse. Such quantum beats between excitons have already been observed in GaN.[21] To prove this, the relative phase of these beats has been probed for several excitation energies across the A and B exciton resonances. No phase shift was observed, confirming their assignment to the coherent superposition of the A and B excitonic responses. The period T of the beats corresponds exactly to the energy splitting ΔE between the A and B excitons (for example, $T=0.8$ ps for sample S_7 corresponds to $\Delta E=5$ meV and $T=0.5$ ps for sample S_1 corresponds to $\Delta E=8$ meV). As such, this period is directly affected by the value of the biaxial stress in the layer and decreases when the latter increases. The autocorrelation signal also exhibits a rapid decay which is shown by our modeling to be strongly dependent on the crystal homogeneity: the stronger the inhomogeneous broadening parameter, the shorter the decay time.

At low temperature, the homogeneous broadening is weak in comparison with the inhomogeneous one which governs the damping of the correlation signal. Thus, only two parameters (in addition to the resonance energy E_{0j}, which can be easily estimated from the fit of the cw-reflectivity spectrum) have to be determined: σ_j which characterizes the disorder (it should be smaller for thick freestanding GaN samples than for thin heteroepitaxial ones) and A_j which is proportional to the exciton oscillator strength.[22] A good agreement can be obtained between numerical simulations and experimental cw-reflectivity spectra, but it is difficult to extract independently both the oscillator strength and the inhomogeneous broadening parameters. Our technique consists in fitting both cw and time-resolved reflectivity spectra in order to improve our accuracy. The energy and the oscillator strength (the latter being related to the amplitude of the quantum beats in the time-resolved spectra) of free excitons are extracted from the best fits of cw and time-resolved spectra. The inhomogeneous broadening parameter is directly extracted from the decay rate of the 5 K correlation signal. We have assumed that the exciton line was essentially inhomogeneously broadened at 5 K. Indeed, although the growth techniques are efficient, strain fluctuations are ineluctable in heteroepitaxial GaN. It is, however, effectively difficult to demonstrate that an inhomogeneous model of the dielectric constant [Eq. (2)] leads to a better agreement between the experimental reflectivity spectra and the simulations. It would be necessary to separate the contribution to the whole broadening of the homogeneous and inhomogeneous ones at low temperature, typically 2 K, but it is a hard task. It is worth mentioning the work of Fisher *et al.* who performed femtosecond four-wave mixing studies of excitons in GaN.[21] From an analysis carried out at 10 K, they deduced an upper limit of 1.5 meV for the inhomogeneous broadening in their samples for a total spectral broadening of 2.5 meV. However, their opinion was that the broadening was essentially homogeneous. However, in our case, a mean broadening of about 1.5 meV is found from the fitting of our 5 K data for the various samples investigated here, whatever the model used: inhomogeneous or purely homogeneous ($\sigma_i=0$). The fact that our broadening values are less than 2.5 meV argues in favor that some significant inhomogeneous broadening was present in the samples studied by Fisher *et al.* It is also worth noting that our choice to consider a weak homogeneous broadening at

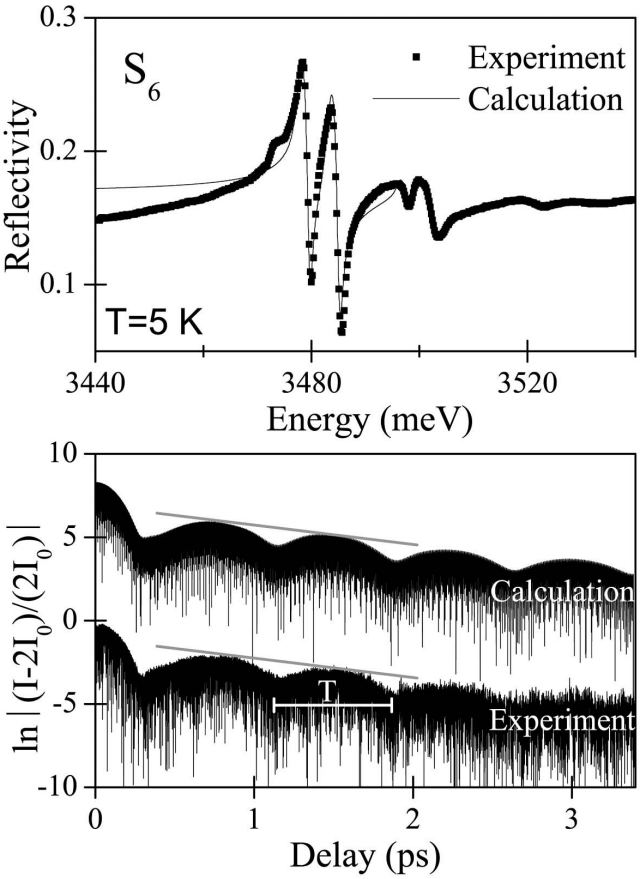

FIG. 3. 5 K continuous-wave and time-resolved autocorrelation reflectivity spectra of sample S_6. The experimental spectra are plotted together with the calculated ones for comparison. In order to outline the good agreement between experiment and calculation, the normalized quantity $\ln|(I-2I_0)/(2I_0)|$ is plotted for the autocorrelation spectra where I is the intensity of the autocorrelation signal and I_0 is the intensity far from the pulse. The period (T) of the excitonic quantum beats, clearly in evidence on the experimental and calculated autocorrelation spectra, is also given.

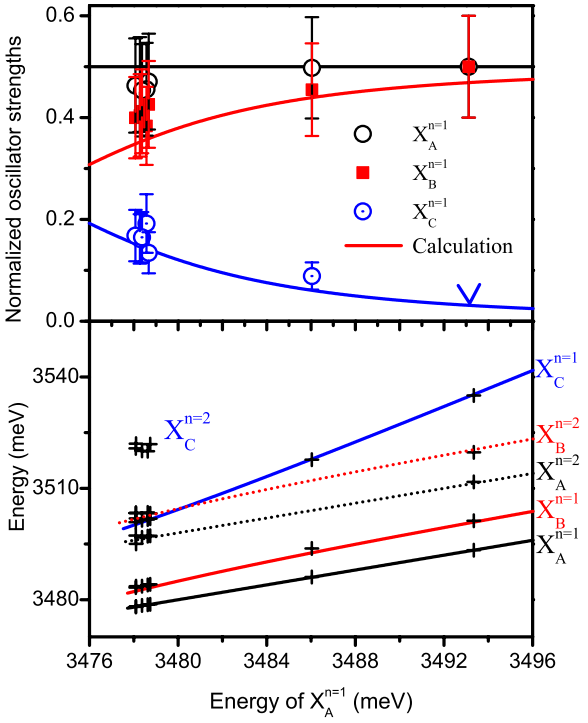

FIG. 4. (Color online) The experimental transition energies and oscillator strengths of the A, B, and C excitons reported as a function of $X_A^{n=1}$ energy are compared with calculations. The symbols correspond to experimental data and the solid lines to calculations using the parameters given in the text. The $\vee$ symbol corresponds to an upper bound for the oscillator strength value of the C exciton in the case of a highly strained GaN sample (S_1).

5 K in the fitting procedure has no influence on the determination of the parameters of the phonon-exciton interaction (Sec. III C) since the temperature-dependent homogeneous broadening is correctly taken into account when the temperature is increased. As an example, Fig. 3 shows that a very good agreement can be obtained between experiments and calculations for both cw and time-resolved spectra at 5 K in the case of sample S_6. The theoretical and experimental correlation spectra have been plotted on a logarithmic scale in order to emphasize the quality of the fit to experimental data. Since only free excitons are taken into account in our model, some discrepancies exist between the experimental and calculated cw-reflectivity spectra observed near the neutral donor bound exciton energy.

B. Excitonic properties as a function of the in-plane biaxial strain

This section is especially devoted to the analysis of the excitonic energies and oscillator strengths as a function of the biaxial residual strain. The experimental data are discussed within theoretical calculations based on Hopfield's model.[23,24] The literature provides a great number of papers on the evolution of experimental excitonic energies as a function of strain and their comparison with theoretical calculations[25–28] but the situation becomes more complicated when it concerns an overall fit of both excitonic energies and oscillator strengths. The excitonic energy and oscillator strength values corresponding to the present analysis are reported in Fig. 4 as a function of the X_A energy, since the latter varies linearly with the in-plane biaxial strain.[26] The value of the unstrained band gap at 5 K was taken equal to 3501 ± 1 meV. It corresponds to an X_A exciton energy of 3477 meV, in agreement with the value determined by Korona *et al.* on GaN homoepitaxial layers grown on GaN single crystals[29] (the values used for the excitonic binding energies are those previously determined in Sec. III A). This unstrained X_A energy agrees with the ones we measure in our thick freestanding samples and the splittings between the X_A, X_B, and X_C energies are only functions of the spin-orbit (Δ_{SO}) and crystal field (Δ_{cr}) parameters of the $\mathbf{k}=0$ wurtzite valence band Hamiltonian.[24] So, in the first step, the X_B and X_C energies of our freestanding samples were fitted at zero strain by varying the Δ_{SO} and Δ_{cr} values and, in the second step, the deformation potentials D_1 and D_2 were adjusted in order to fit the evolution of the excitonic energies as a function of the X_A energy. D_1, D_2, D_3, and D_4 are the usual

deformation potentials defined in Ref. 24; they satisfy the quasicubic approximation, $D_3=D_1-D_2$ and $D_4=-D_3/2$. In order to reduce the number of fitting parameters, the anisotropic property of the wurtzite symmetry was ignored and the deformation potential of the conduction band was fixed to $a_c=a/2=-4.08$ eV, in agreement with the value determined by Gil *et al.*[26] This first evaluation of Δ_{SO}, Δ_{cr}, D_1, and D_2 constituted the starting point of a consistent fit of the whole set of experimental data (i.e., both excitonic energies and oscillator strengths). A good overall agreement was obtained with the following values: $\Delta_{SO}=17.5\pm0.5$ meV, $\Delta_{cr}=13\pm0.5$ meV, $D_1=1.1\pm0.2$ eV, and $D_2=3.7\pm0.2$ eV. They are consistent with those predicted in a few critical works.[8,29–31] This set of parameters enables a perfect fit of the exciton energies but it also leads to a good agreement between the evolution of the experimental oscillator strengths and the theoretical interband transition matrix elements as a function of strain through the X_A energy (Fig. 4). This agreement is satisfactory if we consider the following facts:

(i) For unstrained samples, the fundamental *C* exciton resonance is close to the first excited state of X_B ($n=2$) and this could affect the determination of its oscillator strength during the fitting of the reflectivity spectra.

(ii) The *C* exciton is not excited by the femtosecond pulse since its energy is tuned between the *A* and *B* exciton energies. As such, it does not affect the correlation spectra and, therefore, the determination of its oscillator strength cannot be improved by the fit of the time-resolved reflectivity spectra.

(iii) The calculated oscillator strengths correspond to band-to-band processes through the determination of the strain-dependent optical matrix element for a polarization perpendicular to the *c* axis and the excitonic exchange interaction was not considered. In our experimental configuration, three Γ_5 exciton states are optically active, but the effects of the exchange interaction are weak, especially since we studied relaxed or biaxially compressed samples, i.e., far from the *A* and *B* Γ_5 exciton anticrossing.[32]

(iv) The *C* exciton energy is equal to the energy of optical transitions involving conduction band and *A* valence band ($|\Gamma_9^v\rangle$) continuum states. This effect, known as the Fano effect, certainly affects the determination of the oscillator strength and the associated broadening related to the *C* exciton.

Finally, we found that the ratio of the oscillator strength between the fundamental ($X_A^{n=1}$) and the excited ($X_A^{n=2}$) exciton states varies between 1/7 and 1/10 in our samples, in agreement with the $1/2^3$ factor expected within the hydrogen model. This favorably corroborates our experimental determinations.

Only normalized values of the oscillator strengths are reported in Fig. 4 and are compared with the normalized interband matrix elements calculated as a function of strain. The absolute values of the oscillator strengths can also be given in terms of polarizability ($4\pi\alpha_j$). The latter are related to the quantity A_i used in Eq. (2) by $4\pi\alpha_j E_{0j}^2=A_j$.[33] For the unstrained case, the best fit of our experimental data was obtained using unstrained oscillator strength values ($4\pi\alpha_j$) equal to 2.0×10^{-3} ($A=24\times10^3$ meV^2), 1.6×10^{-3} ($A=20\times10^3$ meV^2), and 0.6×10^{-3} ($A=8\times10^3$ meV^2) for the *A*, *B*, and *C* excitons, respectively. The relative oscillator strength values are then 0.46, 0.39, and 0.15.

C. Temperature-dependent results

The broadening of excitonic lines due to exciton scattering by acoustic and polar optical phonons is investigated in this section. Exciton-phonon interactions are governed by fundamental intrinsic properties and cannot be controlled. Nevertheless, their basic knowledge is very important to estimate the performances of novel devices such as exciton-polariton based light emitters. For example, the broadening induced by the exciton-phonon interaction when the temperature increases is at the origin of the reduction of the Rabi splitting observed in microcavities. Thus, the design of microcavity devices will have to be optimized in order to preserve the strong coupling between photons and excitons at room temperature. Reliable values of the physical parameters characterizing the exciton-phonon interaction are extracted from complementary temperature-dependent cw and time-resolved experiments.

The linewidth of excitons in semiconductors has been theoretically studied by Segall and Mohan using a perturbative approach.[34] Generally, the temperature dependence of the homogeneous linewidth of excitons in semiconductors has the following form:[35]

$$\gamma_{\mathrm{hom}}(T)=\gamma_{ac}T+\gamma_{LO}N_{LO}(T)+\gamma_0. \tag{5}$$

The first term of this equation is due to exciton scattering by acoustic phonons via both the deformation potential and the piezoelectric interaction. The second term arises from exciton interactions with longitudinal optical (LO) phonons via the Frölich interaction which is a Coulomb interaction between excitons and the longitudinal electric field produced by LO phonons.[36] γ_{ac} and γ_{LO} are the exciton-phonon coupling strengths and $N_{LO}(T)$ is the Bose distribution of LO phonons with

$$N_{LO}(T)=1\Big/\left[\exp\left(\frac{\hbar\omega_{LO}}{kT}\right)-1\right],$$

where $\hbar\omega_{LO}=91.8$ meV corresponds to the E_1 mode.[37] The temperature independent term γ_0, which may represent the broadening arising from the scattering by impurities or from the exciton-exciton interactions, has not been considered here.

The method to extract the homogeneous and inhomogeneous linewidths is based on the assumption that the homogeneous broadening is negligible at low temperature in comparison with the inhomogeneous one. In the first step, the inhomogeneous linewidth is obtained from the fit of the low-temperature cw and time-resolved reflectivity spectra. In the second step, the temperature-dependent spectra were fitted by keeping the inhomogeneous broadening constant in order to deduce the homogeneous broadening as a function of temperature.

The temperature-dependent linewidth of excitons in GaN have been determined previously by various spectroscopic

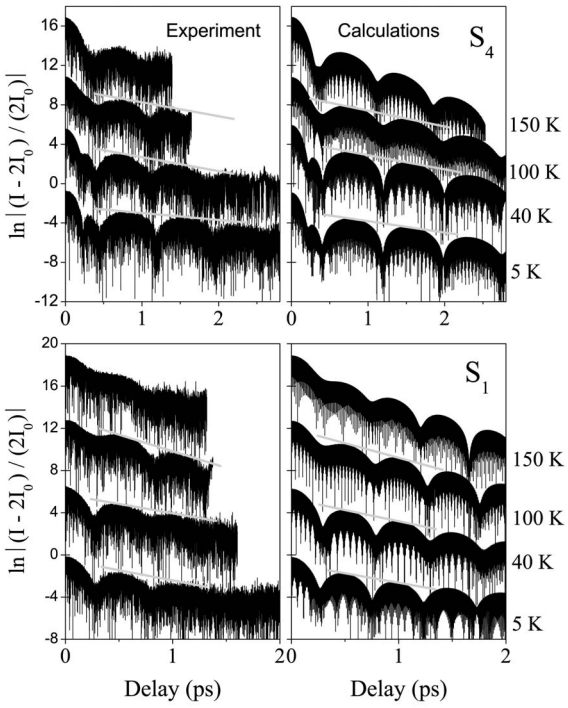

FIG. 5. Series of time-resolved experimental and calculated autocorrelation spectra recorded between 5 and 150 K for samples S_1 and S_4. The decay rate of the time-resolved signal is fitted for each temperature by varying only the homogeneous broadening parameter. The gray straight lines are guides for the eyes highlighting the damping of the correlation signal.

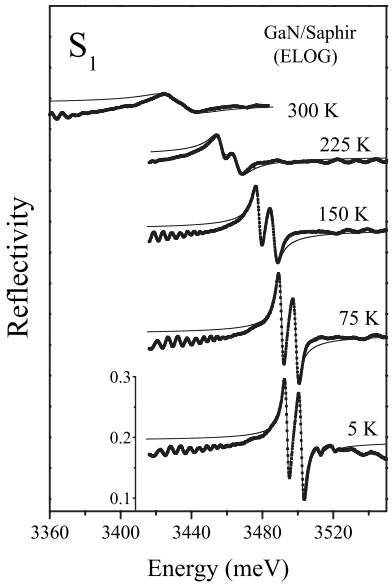

FIG. 6. Series of cw experimental and calculated reflectivity spectra recorded between 5 and 300 K (sample S_1). The fits are consistent with the time-resolved results of Fig. 5.

methods (absorption spectroscopy,[38] photoluminescence,[39] cw-reflectivity,[29,40] and four-wave-mixing studies[21]). In the present work, the strength of the exciton-phonon interaction is determined from the fit of the decay rate of the correlation signal as a function of temperature. The adjustment of simulations to the cw-reflectivity spectra is also performed in order to improve the accuracy of the determination. Moreover, the use of cw-reflectivity data enables us to investigate the whole 5–300 K temperature range, while it is difficult to extract the decay rate of the correlation signal with a good accuracy beyond 150 K. Figure 5 displays the time-resolved spectra together with the calculated ones for samples S_1 (ELOG, highly strained sample) and S_4 (weakly strained freestanding sample) for temperatures varying between 5 and 150 K. Similar results have been obtained for the other samples. The coherence between experiments and calculations is confirmed by the fit of the cw-reflectivity spectra obtained with the same fitting parameters as shown in Fig. 6 for sample S_1. The homogeneous broadening used in this work at 5 K is negligible in comparison with the inhomogeneous one. Its value (0.1 meV) is in good agreement with the lifetime of excitons measured at low temperature in GaN epilayers by Hess *et al.*, who found that the exciton dynamics are dominated by trapping at defects and impurities via acoustic phonons with a lifetime τ of 16 ps.[13] Such lifetime corresponds to a broadening equal to $2\hbar/\tau$=0.08 meV, in agreement with our hypothesis. Moreover, it is worth mentioning that the theoretical description of excitons in semiconductors is well established in the two extreme cases: the case of free excitons where exciton polaritons are formed and that of bound excitons.[22] In the first case, radiative decay of free excitons can only occur through the conversion of polaritons into photons at the surface of the sample. The geometry of the sample governs then the radiative lifetime of exciton polaritons which is related to the confinement of the polariton in the sample. In the second situation, the radiative lifetime of bound excitons is inversely proportional to the oscillator strength. Otherwise, the theory in the intermediate case, which seems to be the case of GaN, does not exist at the present time.

The homogeneous linewidths extracted from the temperature-dependent dephasing rate of the time-resolved reflectivity signal below 175 K and from the fit of cw-reflectivity spectra above 175 K are plotted in Fig. 7. The fact that the slope is linear up to 120 K demonstrates that exciton scattering by acoustic phonons is the dominant scat-

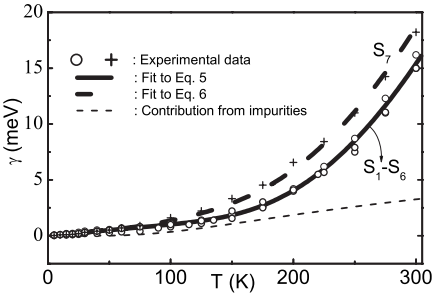

FIG. 7. Homogeneous broadening of the *A* and *B* free excitons in GaN plotted as a function of temperature. The solid lines represent the least-squares fit to Eq. (5) for samples S_1 to S_6 (acoustic phonon and LO-phonon, scattering) or to Eq. (6) (acoustic phonon, LO-phonon, and impurity scattering) in the case of sample S_7.

tering process of excitons in this temperature range. Above 120 K, the homogeneous linewidth becomes superlinear due to the contribution of the optical phonons. The results for samples S_1 to S_6 were fitted with Eq. (5) using the following parameters: $\gamma_{ac}=10\pm2$ μeV K^{-1} and $\gamma_{LO}=420\pm40$ meV. The large deformation potential interaction in addition to the Frölich interaction is responsible for the large value of γ_{LO}, in comparison to the corresponding values obtained for GaAs or ZnSe materials. This could affect the room temperature or high-temperature performances of GaN-based devices. Our determinations have to be compared to those given in the literature and obtained from a large variety of spectroscopic methods.[21,29,38–43] However, care must be taken for this comparison since the inhomogeneous broadening, which is important in GaN samples, may alter the determination of the homogeneous linewidth. For samples with a significant inhomogeneous broadening, the homogeneous linewidth value has to be determined by fitting the excitonic line with a temperature-dependent Lorentzian convoluted with a Gaussian, as done in this work. Approximate expressions have been used in the literature to extract $\gamma_{\mathrm{hom}}(T)$ from the measurements of the whole exciton linewidth Γ_{tot}, either $\Gamma_{tot}^2=\Gamma_{inh}^2+\gamma_{\mathrm{hom}}^2(T)$ (Refs. 44 and 45) or $\Gamma_{tot}=\Gamma_{inh}+\gamma_{\mathrm{hom}}(T)$,[40,41,43] where the inhomogeneous broadening parameter (Γ_{inh}) is measured at low temperature. These relations are inaccurate for highly inhomogeneous broadened excitons and can alter the analysis of the experimental linewidths. Moreover, it can be noted that the literature values found within a similar model can depend on the experimental method. Errors can also be generated during the fitting session. Despite all these sources of discrepancies, our values are very close to those obtained by spectrally resolved and time-integrated four-wave-mixing measurements which provide perhaps the most accurate exciton-phonon coupling parameter determination since the contribution of free carriers is significantly reduced.[21]

As shown in Fig. 7, sample S_7 displays a slightly different temperature-dependent behavior and it was difficult to obtain the same fitting parameters as for the other samples. An impurity (donors) concentration larger than in the other samples certainly explains why the homogeneous broadening parameter of sample S_7 increases faster with increasing temperature. Therefore, to account for the scattering of excitons by ionized impurities, the phenomenological term used by Lee *et al.*[46] is introduced. The homogeneous broadening in Eq. (5) must then be rewritten by adding the contribution of this third scattering mechanism (γ_0 is neglected):

$$\gamma(T)=\gamma_{ac}T+\gamma_{LO}N_{LO}(T)+\Gamma_{imp}e^{-\langle E_b\rangle/kT}, \tag{6}$$

where E_b is the donor binding energy and Γ_{imp} a parameter to be adjusted. The value of $\langle E_b\rangle$ was taken to be equal to 29 meV, which corresponds to an averaged value over all possible donor-impurity binding energies.[47] In Fig. 7, the least-squares fit with Eq. (6) of sample S_7 data is reported using $\Gamma_{imp}=10\pm2$ meV, γ_{ac} and γ_{LO} having been deduced from the analysis of samples S_1 to S_6.

IV. CONCLUSION

Continuous-wave and femtosecond time-resolved autocorrelation reflectivity measurements have been performed on high quality GaN epilayers. Quantum beats between the *A* and *B* excitons were observed and it was shown that the quantum beat period depends on the residual strain through the *A*-*B* splitting energy. The combined analysis of cw and time-resolved reflectivity spectra leads to an accurate determination of the excitonic parameters through the fit of the experimental spectra by using a model allowing a separate estimation of the inhomogeneous and homogeneous broadenings. The evolution of energies and oscillator strengths of the *A*, *B*, and *C* excitons has been studied as a function of the biaxial strain and relevant parameters related to the valence band structure are derived. Finally, the exciton-phonon interaction was studied using temperature-dependent measurements. The phonon-exciton interaction parameters were deduced from the exciton linewidths of cw spectra and from the evolution of the dephasing rate in time-resolved spectra.

[1] S. Nakamura and G. Fasol, *The Blue Laser Diode* (Springer, Berlin, 1997).

[2] B. Gil, in *Group III Nitride Semiconductor Compounds: Physics and Applications*, edited by B. Gil (Oxford University Press, New York, 1998).

[3] A. Khan, M. Chen, Q. Shur, M. S. Dermott, B. T. Higgins, J. A. Burm, J. Schaff, and W. J. Eastman, IEEE Electron Device Lett. **17**, 584 (1996).

[4] M. Saba, C. Ciuti, J. Bloch, V. Thierry-Mieg, R. André, Le Si Dang, S. Kundermann, A. Mura, G. Bongiovanni, J. L. Staehli, and B. Deveaud, Nature (London) **414**, 731 (2001).

[5] P. G. Savvidis, J. J. Baumberg, R. M. Stevenson, M. S. Skolnick, D. M. Whittaker, and J. S. Roberts, Phys. Rev. Lett. **84**, 1547 (2000).

[6] G. Malpuech, A. Di Carlo, A. Kavokin, J. J. Baumberg, M. Zamfirescu, and P. Lugli, Appl. Phys. Lett. **81**, 412 (2002).

[7] B. Gil, S. Clur, and O. Briot, Solid State Commun. **104**, 267 (1997).

[8] R. Stepniewski, K. P. Korona, A. Wysmolek, J. M. Baranowski, K. Pakula, M. Potemski, G. Martinez, I. Grzegory, and S. Porowski, Phys. Rev. B **56**, 15151 (1997).

[9] A. Kavokin and B. Gil, Appl. Phys. Lett. **72**, 2880 (1998).

[10] N. Antoine-Vincent, F. Natali, D. Byrne, A. Vasson, P. Disseix, J. Leymarie, M. Leroux, F. Semond, and J. Massies, Phys. Rev. B **68**, 153313 (2003).

[11] F. Semond, I. R. Sellers, F. Natali, D. Byrne, M. Leroux, J. Massies, N. Ollier, J. Leymarie, P. Disseix, and A. Vasson, Appl. Phys. Lett. **87**, 021102 (2005).

[12] I. R. Sellers, F. Semond, M. Leroux, J. Massies, P. Disseix, A. L. Henneghien, J. Leymarie, and A. Vasson, Phys. Rev. B **73**, 033304 (2006).

[13] S. Hess, F. Walraet, R. A. Taylor, J. F. Ryan, B. Beaumont, and P. Gibart, Phys. Rev. B **58**, R15973 (1998).

[14] J. J. Baumberg, A. P. Heberle, A. V. Kavokin, M. R. Vladimirova,

and K. Kohler, Phys. Rev. Lett. **80**, 3567 (1998).
[15] M. Colocci, F. Bogani, S. Ceccherini, and M. Gurioli, J. Nonlinear Opt. Phys. Mater. **7**, 215 (1998).
[16] M. Gurioli, F. Bogani, S. Ceccherini, and M. Colocci, Phys. Rev. Lett. **78**, 3205 (1997).
[17] B. Beaumont, M. Vaille, G. Nataf, A. Bouille, J. C. Guillaume, P. Vennegues, S. Haffouz, and P. Gibart, MRS Internet J. Nitride Semicond. Res. **3**, 20 (1998).
[18] P. Vennegues, B. Beaumont, V. Bousquet, M. Vaille, and P. Gibart, J. Appl. Phys. **87**, 4175 (2000).
[19] O. Aoude, P. Disseix, J. Leymarie, A. Vasson, E. Aujol, and B. Beaumont, Superlattices Microstruct. **36**, 607 (2004).
[20] M. Zamfirescu, B. Gil, N. Grandjean, G. Malpuech, A. Kavokin, P. Bigenwald, and J. Massies, Phys. Rev. B **64**, 121304(R) (2001).
[21] A. J. Fischer, W. Shan, G. H. Park, J. J. Song, D. S. Kim, D. S. Yee, R. Horning, and B. Goldenberg, Phys. Rev. B **56**, 1077 (1997).
[22] L. C. Andreani, in *Confined Electrons and Photons*, edited by E. Bunstein and C. Weisbuch (Plenum Press, New York, 1995), p. 57.
[23] J. J. Hopfield, J. Phys. Chem. Solids **15**, 97 (1960).
[24] S. L. Chuang and C. S. Chang, Phys. Rev. B **54**, 2491 (1996).
[25] M. Tchounkeu, O. Briot, B. Gil, J. P. Alexis, and R. L. Aulombard, J. Appl. Phys. **80**, 5352 (1996).
[26] B. Gil, O. Briot, and R. L. Aulombard, Phys. Rev. B **52**, R17028 (1995).
[27] A. Alemu, B. Gil, M. Julier, and S. Nakamura, Phys. Rev. B **57**, 3761 (1998).
[28] H. Lahreche, M. Leroux, M. Laugt, M. Vaille, B. Beaumont, and P. Gibart, J. Appl. Phys. **87**, 577 (2000).
[29] K. P. Korona, A. Wysmolek, K. Pakula, R. Stepniewski, J. M. Baranowski, I. Grzegory, B. Lucznik, M. Wroblewski, and S. Porowski, Appl. Phys. Lett. **69**, 788 (1996).
[30] K. Kornitzer, T. Ebner, K. Thonke, R. Sauer, C. Kirchner, V. Schwegler, M. Kamp, M. Leszczynski, I. Grzegory, and S. Porowski, Phys. Rev. B **60**, 1471 (1999).
[31] B. Gil, in *GaN (II)*, edited by J. Pankove and T. Moutsakas (Academic, New York, 1999), Vol. 57, p. 209.
[32] B. Gil and O. Briot, Phys. Rev. B **55**, 2530 (1997).
[33] J. J. Hopfield, Phys. Rev. **112**, 1555 (1958).
[34] B. Segall and G. D. Mahan, Phys. Rev. **171**, 935 (1968).
[35] B. Segall, in *Proceedings of the Ninth Conference on the Physics of Semiconductors*, 1968, edited by S. M. Ryvkin (Nauka, Leningrad, 1968), p. 425.
[36] H. Fröhlich, in *Polarons and Excitons*, edited by C. G. Kuper and G. D. Whitfield (Plenum, New York, 1963), p. 1.
[37] T. Azuhata, T. Matsunaga, K. Shimad, K. Yoshida, T. Sota, K. Suzuki, and S. Nakamura, Physica B **219-220**, 493 (1996).
[38] A. J. Fischer, W. Shan, J. J. Song, Y. C. Chang, R. Horning, and B. Goldenberg, Appl. Phys. Lett. **71**, 1981 (1997).
[39] S. Chichibu, H. Okumura, S. Nakamura, G. Feuillet, T. Azuhata, T. Sota, and S. Yoshida, Jpn. J. Appl. Phys., Part 1 **36**, 1976 (1997).
[40] L. Siozade, S. Colard, M. Mihailovic, J. Leymarie, A. Vasson, N. Grandjean, M. Leroux, and J. Massies, Jpn. J. Appl. Phys., Part 1 **39**, 20 (2000).
[41] C. F. Li, Y. S. Huang, L. Malikova, and F. H. Pollak, Phys. Rev. B **55**, 9251 (1997).
[42] J. Petalas, S. Logothetidis, S. Boultadakis, M. Alouani, and J. M. Wills, Phys. Rev. B **52**, 8082 (1995).
[43] A. K. Viswanath, J. I. Lee, D. Kim, C. R. Lee, and J. Y. Leem, Phys. Rev. B **58**, 16333 (1998).
[44] D. Gammon, S. Rudin, T. L. Reinecke, D. S. Katzer, and C. S. Kyono, Phys. Rev. B **51**, 16785 (1995).
[45] Y. Chen, G. P. Kothiyal, J. Singh, and P. K. Bhattacharya, Superlattices Microstruct. **3**, 657 (1987).
[46] J. Lee, E. S. Koteles, and M. O. Vassell, Phys. Rev. B **33**, 5512 (1986).
[47] A. Wysmolek, K. P. Korona, R. Stepniewski, J. M. Baranowski, J. Bloniarz, M. Potemski, R. L. Jones, D. C. Look, J. Kuhl, S. S. Park, and S. K. Lee, Phys. Rev. B **66**, 245317 (2002).